JOURNAL OF MATERIALS SCIENCE 33 (1998) 429–433

Preparation and high-temperature behaviour of electrolytic alumina film on Fe–Cr–Al stainless steel

L. ARIES, J. ROY, S. EL HAJJAJI*, L. ALBERICH, P. VICENTE HERNANDEZ
Equipe de Métallurgie Physique – Laboratoire des Matériaux (UPRESA CNRS 5071), Ecole Nationale Supérieure de Chimie (INPT), 118 route de Narbonne, 31077 Toulouse Cedex, France

P. COSTESEQUE, T. AIGOUY
Equipe Minéralogie et Cristallographie – LMTG (UMR CNRS 5563), Université Paul Sabatier, 39 allées Jules Guesde, 31000 Toulouse, France

Fe–23 Cr–5Al stainless steel was functionalized by a conversion treatment in order to allow alumina electrodeposition with strong interfacial bonding. The very porous conversion coating prepared in acid solution had excellent adhesion and was conductive enough to permit cathodic reactions inducing local pH conditions favourable for the precipitation of alumina oxyhydroxide during electrolysis of aluminium salt solutions. The coating presented chemical composition gradients suitable for strong adhesion. The improvement of the thermal oxidation behaviour was studied at 1000 °C

1. Introduction

Ceramic coatings are widely used to protect materials, particularly metals and alloys, against oxidation at high temperature [1–15]. Problems are the adhesion and the thermal shock resistance of the coat. In previous papers [16, 17], a method to obtain adherent ceramic film on stainless steels and superalloys, by electrochemical means has been described. This method involves a pretreatment which leads to the formation of a functional conversion coating to a strong interfacial adhesion with the substrate and a particular morphology.

During the first step of this method, the metal surface is functionalized by a conversion treatment carried out in an acid solution with suitable additives. The second step corresponds to the electrodeposition of oxides or oxyhydroxides. The thickness and composition of the coatings are easily controlled, even on complex shapes, by varying electrochemical parameters and bath composition. The third step consists of heating to dehydrate the coat and induce interfacial reactions between the compounds of the conversion coatings and those of the electrolytic deposit. So, a refractory character is conferred on the surface at high temperature.

Note that the conversion coating obtained after pretreatment must be microporous to allow the deposit of refractory oxide or oxyhydroxide by electrolysis. It contributes to the "anchoring" of the ceramic layer and facilitates interfacial reactions during the last step of the process.

For Fe–17%Cr stainless steel, it has been demonstrated [18] that the conductive conversion coating, owing to its particular morphology with pores and cavities, facilitates the reduction reactions responsible for the increase of the pH at the surface and acts as a porous electrode allowing local pH conditions favourable for aluminium oxyhydroxide precipitation.

For applications involving high temperatures, the use of Fe–Cr–Al stainless steel is of great interest. Conversion coatings on Fe–Cr–Al alloys for solar absorbers [19] and catalysis [20] have been described and their thermal stability studied up to 1000 °C. The aim of the present work is to study the effect of aluminium on the characteristics of the conversion coating and especially on its capacity to induce the precipitation of aluminium hydroxide by electrolysis. Electrochemical coat composition and thermal resistance aspects of the alumina coating on Fe–Cr–Al alloy are presented.

2. Experimental procedure

The composition of the Fe–Cr–Al alloy is given in Table I. The specimen dimensions were 0.6 mm × 20 mm × 50 mm. Original conversion coatings of such stainless steels can be obtained by a method described elsewhere [21], either by electrolytic treatment or chemical treatment in an acid bath containing suitable additives.

Present address: Laboratoire de Chimie Physique Appliquée (Section Electrochimie – corrosion), Departement de Chimie, Av Ilon Batouta, BP1014, Rabat, Morocco.

0022–2461

TABLE I Chemical composition (wt%) of the stainless steels used

Cr	Al	Si	Mn	Ni	Mo	P	C	Ti	Zr	Y	Fe
23.20	5.12	0.23	0.25	0.36	< 0.01	0.015	0.08	0.21	0.135	0.055	Bal.

In the present study, conversion coatings were obtained by chemical treatment at 60 °C in sulfuric acid solution (15 vol% H_2SO_4) containing 1.6×10^{-2} mol l^{-1} sodium thiosulfate and 0.4 mol l^{-1} propargyl alcohol used as corrosion inhibitor. The electrode potential of the stainless steel during the conversion treatment was measured using a voltmeter and a saturated calomel electrode as reference.

Cathodic deposition of alumina was performed at 15 °C with an aqueous solution of aluminium sulfate ($Al_2(SO_4)_3 \cdot 14H_2O$, 350 g l^{-1}), using a platinum electrode as anode. Polarization curves were obtained using a potentiostat fitted with a pilot scanner (10 mV min^{-1}).

The coatings were analysed by SIMS using an IMS 300 Cameca analyser (analysed zone about 25 μm diameter). X-ray diffraction was carried out *in situ* on the metal substrate using a PW 1011 Philips diffractometer.

Isothermal oxidation experiments were carried out in dynamic oxygen for 12 h at 1000 °C, under atmospheric pressure. The weight gain of the specimens was determined with a SETARAM TAG 24 S thermobalance with two symetrical furnaces.

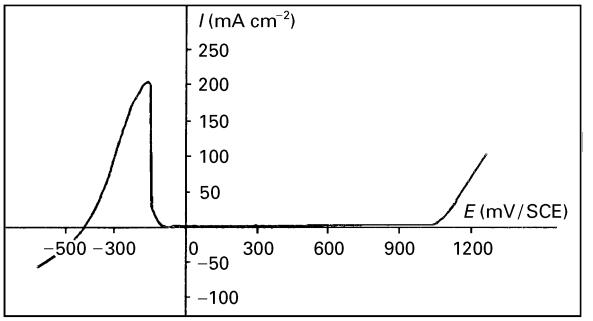

Figure 1 Polarization curve for Fe–Cr–Al alloy in the treatment bath.

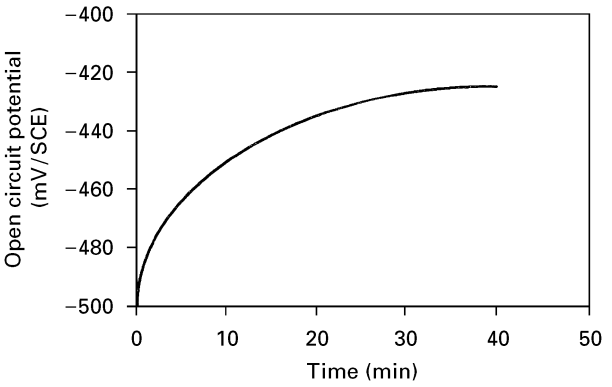

Figure 2 Electrode potential against treatment time.

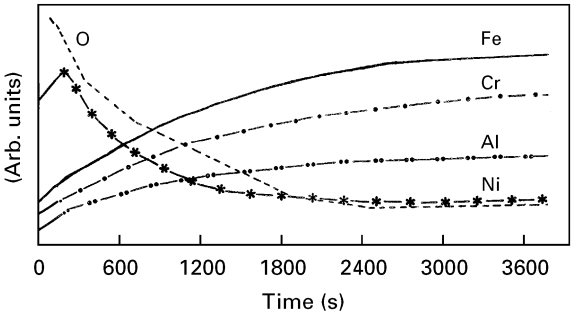

Figure 3 Distribution profiles of the elements in the initial conversion coating against bombardment time.

3. Results

3.1. Chemical conversion coating

3.1.1. Preparation

The polarization curve of the Fe–23%Cr–5%Al stainless steel in the conversion treatment bath at 60 °C is shown in Fig. 1. The corrosion potential was about − 440 mV while the passivation potential was near − 140 mV. The activity peak with current densities reaching 230 mA cm^{-2} is followed by a large passivity domain where current densities are in the range of 10 mA cm^{-2}. Such high passivity current density associated with a broad corrosion domain, shows that the layer grown on the stainless steel was not very protective. So, the preparation of the conversion coating was possible by dipping the steel into a bath (chemical treatment), the electrolytic route at a potential corresponding to the activity domain was not necessary. Nevertheless, to facilitate conversion coating formation, cathodic activation treatment of the surface was carried out with a current generator and a platinum counter-electrode as anode for a few seconds; the activation potential was about − 1 V. The aim of this cathodic treatment was to suppress the thin layer of naturally formed oxide on the stainless steel surface.

Fig. 2 shows the electrode potential variation of a sample dipped into the bath, during the conversion treatment. After the cathodic activation period, the potential stabilized at values about − 440 mV, i.e., near the corrosion potential in the active state measured on polarization curves. During the treatment, the electrode potential increased very slowly, corresponding to the growth of the conversion coating which acts as a barrier between the steel surface and the solution.

3.1.2. Chemical composition

SIMS analysis (Fig. 3) of iron, chromium and aluminium giving identical profiles suggests that they are part of the same chemical compound. Using infrared spectrometery and X-ray diffraction, in a previous work [22], it was shown that the main component of this kind of coating is a substituted magnetite $(Fe^{2+}Fe^{3+}_{2-x-y}Cr^{3+}_{x}Al^{3+}_{y})O_4$ with varying degrees of

oxidation, according to the depth in the coat. Moreover, the preparation of the conversion coating leads to a slight enrichment in nickel, probably in the oxidized state.

Conversion coating thickness was evaluated at about 200 nm from the sputtering time under ionic bombardment (SIMS).

3.2. Electrodeposition of aluminium hydroxide

3.2.1. Preparation

Cathodic polarization curves for the Fe–23%Cr–5%Al steel with and without the conversion coating, in the aqueous solution of aluminium sulfate at 15 °C are shown in Fig. 4.

In the case of the uncoated stainless steel, the cathodic current increased quickly from − 1.2 V up to − 3.4 V, this potential domain being fitted with hydrogen evolution at the steel surface. So, because the very weak current densities given by the reduction of dissolved oxygen, are not detectable on the polarization curve, the main electrochemical reaction taking place is the reduction of protons to form hydrogen. At very low potentials (high current densities), a decrease or stagnation of the current versus potential was observed because of the formation of a thick non-adherent deposit insulating the metal surface and slowing down the rate of proton reduction.

In the case of the stainless steel covered by conversion coating (Fig. 4), the current densities increased from a potential higher than that noted for the uncoated steel (− 0.8 V instead of − 1.2 V). This different behaviour is attributed to the composition and special morphology of the conversion coating; in particular, the surface roughness of the coating can decrease the proton reduction overpotential and make hydrogen release easier. Between − 1 and − 1.7 V the polarization curve presented a plateau, characteristic of a diffusional phenomenon, probably associated with the diffusion of electroactive species into pores of the conversion coating and into the aluminium hydroxide deposit. From − 1.7 to − 3.1 V the polarization regime is similar to that observed for the uncoated steel, because the conversion coating is covered with a hydroxide deposit blocking the pores of the initial coating. At very low potential the current seems to be limited, fluctuations and even current drops can be observed because of the insulating character of the deposit which is damaged to varying degrees by gas bubbles.

Deposits were obtained at constant potential fixed at − 4 V. First the coating weight increased quickly with deposition time, then it stabilized (Fig. 5) after 40 min. The current densities maintained high values during deposition (Fig. 6) because of the weak insulating character of the deposit; in the same way, the cell voltage between anode and cathode was almost constant during the growth of the deposit (Fig. 6). For a deposition time fixed at 40 min, the coating weight increased with cathodic potential, the weight of deposit being significant from − 1 V (Fig. 7); Fig. 8 indicates that the cell voltage and electrolysis current at the end of the treatment (after 40 min) was dependent upon the applied cathodic potential.

3.2.2. Thermal behaviour

The samples were heated in air for 5 h at 350, 650, 800, 900 and 1000 °C. The structural variation of the coating can be compared to the growth of oxides on

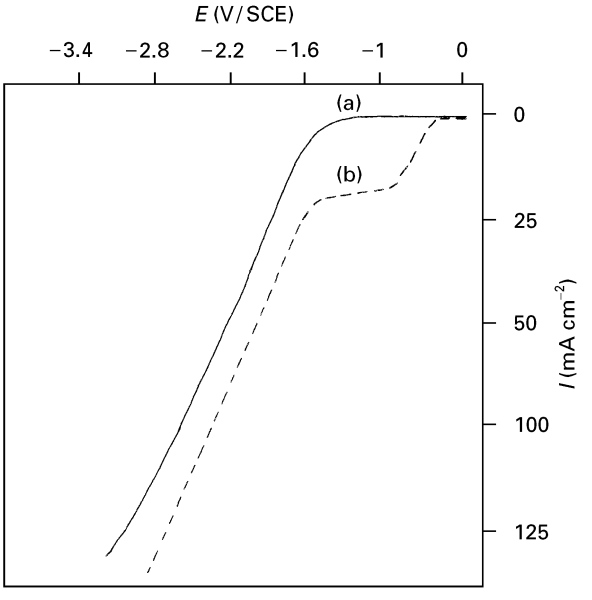

Figure 4 Polarization curves of (a) uncoated steel and (b) coated steel in the aluminium sulfate bath.

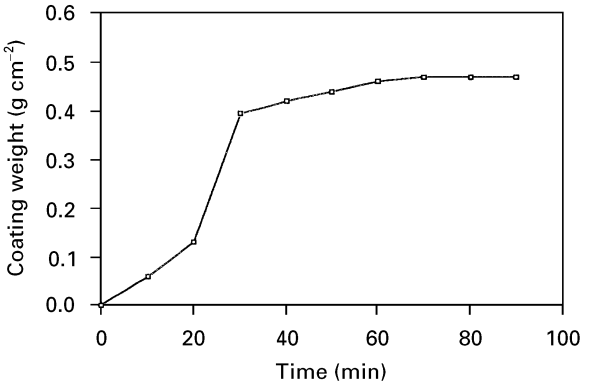

Figure 5 Coating weight versus deposition time at a potential of − 4 V in an aluminium sulfate bath.

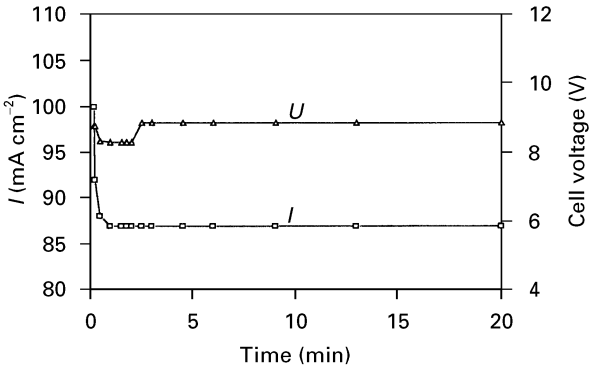

Figure 6 Current density and cell voltage versus deposition time in an aluminium sulfate bath.

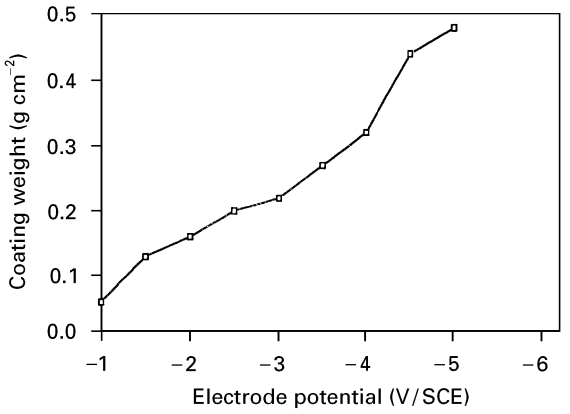

Figure 7 Coating weight versus electrode potential in the aluminium sulfate bath.

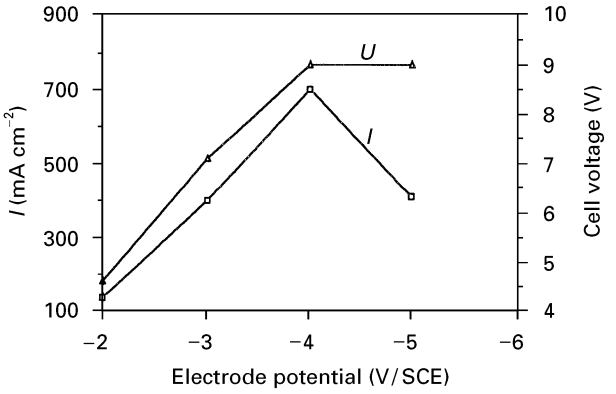

Figure 8 Current density versus electrode potential in the aluminium sulfate bath.

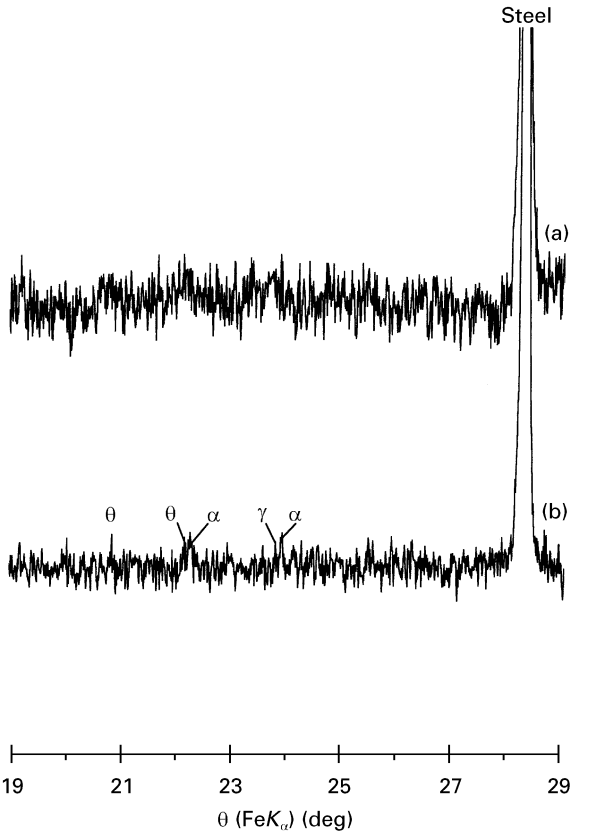

Figure 9 X-ray diffraction spectra of (a) uncoated steel and (b) coated steel after heat treatment at 900 °C. α, α-Al_2O_3; γ, γ-Al_2O_3; θ, θ-Al_2O_3.

the Fe23Cr5Al steel by thermal oxidation in air during the same time.

After heat treatment, X-ray diffraction analyses of the coatings on the metal substrate were performed.

From 350–800 °C, the diffractograms of coated and uncoated steel show only the peaks of a Fe–Cr–Al solid solution corresponding to the steel, the oxide phases of the layer being amorphous or weakly crystallized. At 900 °C, only some weak peaks of transition aluminas were seen (Fig. 9), the aluminas being practically amorphous. At 1000 °C (Fig. 10), the uncoated steel diffraction spectrum shows fine peaks of α-alumina resulting from the steel oxidation phenomenon. On the other hand, the diffraction spectrum of the coated steel shows less fine and smaller peaks of α- and γ-alumina (poorly crystallized) which can be attributed to phase transformation in the coating. This result shows that the coat prevents the formation of the well-crystallized α-alumina coming from the substrate; it acts as a barrier and so protects the steel against oxidation. It is very probable that the thickness of the deposit limits exchanges between the superficial pure aluminas and the steel, the absence of impurity hindering the crystallization of the aluminas.

The mixed oxides $(Fe^{2+}Fe^{3+}_{2-x-y}Al^{3+}_x Cr^{3+}_y)O_4$ formed at the interface by the reaction between the steel conversion coating and the deposit, observed with an Fe–Cr substrate [18] are not perceptible, probably

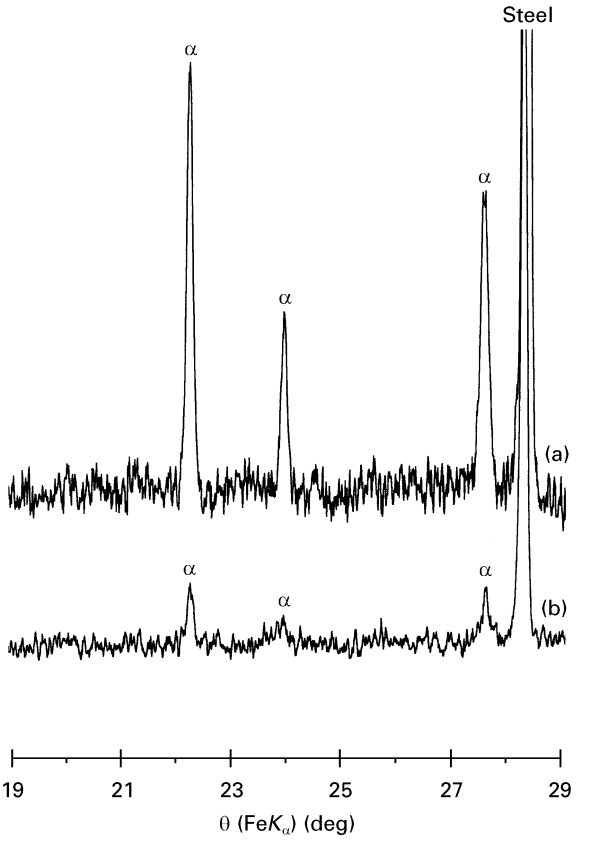

Figure 10 X-ray diffraction spectra of (a) uncoated steel and (b) coated steel after heat treatment at 1000 °C. α, α-Al_2O_3; γ, γ-Al_2O_3.

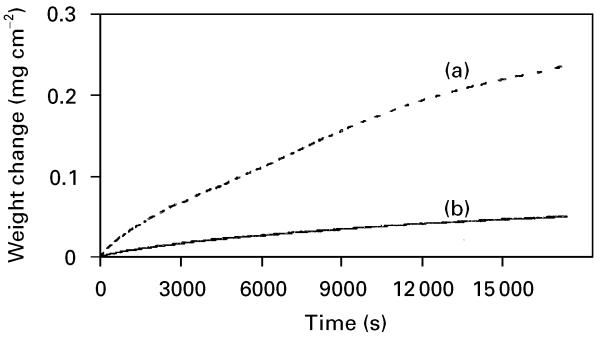

Figure 11 Weight gain of (a) uncoated steel and (b) coated steel against time in oxygen at 1000 °C.

because the interface is too thin compared to the thick alumina deposit. This interface, with a concentration gradient varying according to the depth, plays a decisive role in coat adhesion [16, 17].

A high-temperature oxidation was carried out in dynamic oxygen at 1000 °C for 12 h. Fig. 11 shows the weight change versus time curves for the uncoated and coated Fe–Cr–Al alloy specimens. The coated alloy exhibits a low oxidation rate compared to that of the uncoated alloy owing to the thickness and adhesiveness of the poorly crystallized alumina coating. This result agrees with the protective character of the coating.

4. Conclusion

The behaviour of Fe–Cr–Al stainless steel functionalized by a chemical conversion treatment in acid solution, is similar to that of Fe–Cr stainless steel. The conversion coating is mainly composed of an aluminium, chromium-substituted magnetite. This coat is conductive and porous enough to permit, during the electrolysis of aluminium salt aqueous solutions, cathode reactions including local pH conditions favourable for the precipitation of aluminium oxyhydroxide on to its surface and into the pores. The presence of aluminium in the alloy does not greatly affect the electrode properties or the morphology of the conversion coating.

After dehydration by heating, the refractory coating is made of alumina at the surface and mixed oxides in the inner layer. The coat modifies the oxidation kinetics of the alloy and its thermal oxidation behaviour, decreasing the oxidation rate and the scaling phenomena observed for Fe–Cr–Al alloys at very high temperatures. So, the proposed method, which involves chemical conversion treatment prior to the electrolytic deposit, can be effectively used to prepare ceramic coatings on alloys.

References

1. J. A. SWITZER, *J. Electrochem. Soc.* **133** (1986) 722.
2. *Idem*, *Amer. Ceram. Soc. Bull.* **66** (1987) 1521.
3. H. KONNO, *J. Electrochem. Soc.* **134** (1987) 1034.
4. D. E. CLARK, W. J. DALZELL and D. C. FOLZ, *Ceram. Engng Sci. Proc.* **9** (1988) 1111.
5. T. E. SCHMID and R. Y. HECHT, *ibid.* **9** (1988) 1089.
6. H. KONNO and R. FURUICHI, *J. Met. Finish. Soc. Jpn* **39** (1988) 29.
7. L. GAL-OR, I. SILBERMAN and R. CHAIM, *J. Electrochem. Soc.* **138** (1991).
8. R. CHAIM, I. SILBERMAN and I. GAL-OR, *ibid.* **138** (1991) 1942.
9. C. R. AITA, *Mater. Sci. Technol.* **8** (1992) 666.
10. N. K. HUANG, H. KHEYRANDISH and J. S. COLLIGON, *Phys. Status. Solidi.* (*a*) **132** (1992) 405.
11. H. KONNO, M. TOKITA, A. FURUSAKI and R. FURUICHI, *Electrochem. Acta.* **37** (1992) 2421.
12. M. ATIK, J. ZARZYCKI and C. R'KHA, *J. Mater. Sci. Lett.* **13** (1994) 266.
13. R. CHAIM, G. STARK and L. GAL-OR, *ibid.* **13** (1994) 487.
14. R. CHAIM, G. STARK, L. GAL-OR and H. BESTGEN, *J. Mater Sci.* **29** (1994) 6241.
15. I. ZHITOMIRSKY, L. GAL-OR, A. KOHN and H. W. HENNICKE, *ibid.* **30** (1995) 5307.
16. L. ARIES, *J. Appl. Electrochem.* **24** (1994) 554.
17. L. ARIES and F. DABOSI, Brevet INPT Fr. 9312 790 (1993).
18. L. ARIES, J. ROY, J. SOTOUL, V. PONTET, P. COSTESEQUE and T. AIGOUY, *J. Appl. Electrochem.* **26** (1996) 617.
19. L. ARIES, M. EL BAKKOURI, J. ROY, J. P. TRAVERSE, R. CALSOU and R. SEMPERE, *Thin Solid Films* **197** (1991) 143.
20. L. ARIES and J. ROY, *Mater. Sci. Technol.* **10** (1994) 359.
21. L. ARIES, R. CALSOU, J. A. FLORES and J. ROY, *Br. Corros. J.* **25** (1990) 299.
22. L. ARIES, J. ROY, T. BOUISSOU and R. SEMPERE, *Mater. Sci. Technol.* **7** (1991) 24.

Received 17 July 1996
and accepted 22 August 1997